A unified model of power sources for the simulation of electrical energy systems

A Unified Model of Power Sources for the Simulation of Electrical Energy Systems*

Sara Vinco, Yukai Chen, Enrico Macii and Massimo Poncino
Department of Control and Computer Engineering, Politecnico di Torino, Torino, Italy
name.surname@polito.it

ABSTRACT

Models of power sources are essential elements in the simulation of systems that generate, store and manage energy. In spite of the huge difference in power scale, they perform a common function: converting a primary environmental quantity into power. This paper proposes a unified model of a power source that is applicable to any power scale, and that can be derived solely from data contained in the specification or the datasheet of a device. The key feature of our model is the normalization of the energy generation characteristic of the power source by means of a reduction to a function expressing extracted power *vs.* the "scavenged" quantity. The proposed model proved to apply to two kinds of power sources, *i.e.*, a wind turbine and a photovoltaic panel, and to provide a good level of accuracy and simulation performance *w.r.t.* widely adopted models.

Keywords

Electrical Energy Systems; Power simulation; Power source modeling; Datasheet; Electronic design automation

1. INTRODUCTION

Simulation is an essential step in the design of Electrical Energy Systems (EES) for the assessment or the sizing of both the system and its components, as experimenting with EESs or their components is not only time consuming, but sometimes even dangerous due to high voltages or currents.

Among the various components of EESs, the most diverse of all are power sources, *i.e.*, elements that generate power by transforming some environmental quantity in electrical energy. The variety of their characteristics tends in fact to follow the scale of the relative EES: they range from the μW/mW scale of MEMS-based energy micro-scavengers to the MW scale of large wind turbines, and the very scavenging mechanism can be quite different. This variety in their typologies makes their modeling poorly scalable and marginally re-usable, thus complicating the objective of using an as much as possible unified modeling approach. Another difficulty towards a possibly unified view of the models lies in the fact that most works focus on a specific application context (*e.g.*, smart electronic systems, micro-grids, large-scale power grids). Therefore, from their perspective, there is no need of deriving models able to cover multiple energy scales.

The context of our work is the *system-level simulation of an EES* for its early validation and fast assessment through a model-based design scenario [10, 16, 23]. Modeling approaches comparable to ours include functional models suitable for system-level simulation and adopted for early prototyping of large scale systems [10, 30].

Our approach is similar in scope and in the abstraction level to the works of [14] and [19]. Besides some basic differences in the abstract semantics of the models and the languages used for their description, the fundamental distinction between those solutions and ours lies in the *identification of the model parameters*: these works do not describe how the model parameters can be derived for a generic device; the models are described and built for one specific example device and how to extend them to a different instance is not specified. The lack of an identification method implies that the input/output characteristic of the device can be obtained only by resorting to empirical measures of some physical parameters. Needless to say, this is costly and it requires instrumentation that may not always be available in-house. Furthermore, this would restrict exploration of the possible alternatives, as the designer would have to acquire a number of components to estimate the most suitable one. The alternative is to use data provided by the manufacturer together with the power source. However, the latter rarely provides the required information for populating the models, thus preventing the mapping of an abstract model to the specific power source.

The goal of this paper is to derive a *unified model for power sources* that is *applicable to any power scale and to any kind of power source*. Thanks to this unified approach, the model can be derived solely from data available from a specification of the device. The approach is based on a "normalization" of the energy generation characteristic of the power source in terms of a function expressing extracted power *vs.* the environmental scavenged quantity. The model is then used to generate the simulation traces of voltage and current corresponding to the generated harvested power, to allow simulation of the power source in the context of the overall EES. Experimental results have shown a high level of accuracy *w.r.t.* state-of-the art models and a significant simulation speed up, up to 7x.

2. RELATED WORK

The large variety of types of power sources is reflected by the many available options for their modeling. A general classification is outside the scope of this work, and in any case the landscape of

*This work was supported by the EC co-funded CONTREX (Design of embedded mixed-criticality CONTRol systems under consideration of EXtra-functional properties) project Grant Agreement FP7-ICT- 611146

GLSVLSI '16, May 18-20, 2016, Boston, MA, USA

DOI: http://dx.doi.org/10.1145/2902961.2903024

options is so wide that an exhaustive coverage of models for all types of power sources is virtually impossible. A possible generic classification concerns their abstraction level, which typically maps onto a well-defined simulation semantics [23]:

- *multiphysics-based mechanical models* generally focus on the description of the mechanical or fluidic characteristics of the power source, *e.g.*, tools like COMSOL or CoventorWare [7,8];
- *equation-based models* analytically express the physical phenomena that govern the energy generation process [11];
- *electrical circuit equivalent models*, in which the dynamic behavior of electrical components is used to emulate the operation of the device [5,24];
- *functional (continuous or discrete-time) macro-models* suitable for system-level simulation, often specified using hardware description languages [9,29].

Given our system-level, model-based perspective, methods somehow comparable to ours both in scope and in the abstraction level are proposed in [19] and [14]. The models resulting from [19] have an abstraction level similar to ours and are usable in a system-level simulation scenario. However, their derivation is based on the characteristic equations of the specific power sources (*e.g.*, the diode-based equation for a PV cell). [14] provides a more abstract model, in which a power source is modeled as a charge reservoir in which the environment adds and a load draws charge. Although this method goes in the direction of a generalization of the models, the usage in a real scenario (*e.g.*, different load conditions, tracking of maximum power point) is not immediate.

Besides some differences in the abstract semantics of the models, the fundamental distinction between those solutions and ours lies thus in the *identification of the model parameters*: these works do not describe how the model parameters can be derived for a generic device. Conversely, our approach determines a "meta-modeling" procedure that is applicable to any type of power source and relies only on information provided as devices specifications.

3. A UNIFIED MODEL FOR POWER SOURCES

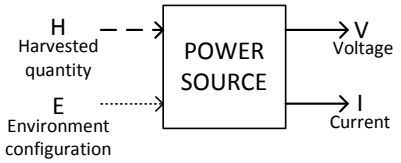

Figure 1: Unified model for power sources.

Any power source can be considered as a system component that generates *voltage and current waveforms over time*, as shown in Figure 1 (signals **V** and **I**). The power produced by the power source strictly depends on the harvested quantity, modeled as an input waveform over time (signal **H**). The power source may be further affected by other environment characteristics, such as temperature (signal **E**). The proposed model is clearly agnostic both of the type of power source (*e.g.*, photovoltaic panel or wind turbine) and of the scale of managed energy (*i.e.*, micro or macro). Our model currently supports power sources that harvest a single environmental quantity (*e.g.*, wind, solar radiation, ambient noise or vibrations). Dependency from other environmental quantities, such as temperature, will be part of future work. The abstraction resulting from the model interface shown in Figure 1 is essential to guarantee the generality and flexibility of the model. In particular, it allows to identify the parameters of the models without requiring any knowledge of instance-specific characteristics of the device, such as the physics of the underlying energy generation process or technological parameters.

Conversely, as mentioned in Section 1, our model can be derived solely from available data contained in specification of the device such as a datasheet. As many types of data can be found, the energy generation characteristic of the power source is *normalized to a canonical form*, in terms of a function expressing *extracted power* vs. *the harvested quantity*. This allows to automate the construction of the power source model and to generate the simulation traces of voltage and current *vs.* the harvested quantity.

4. PROPOSED METHODOLOGY

4.1 Methodology Overview

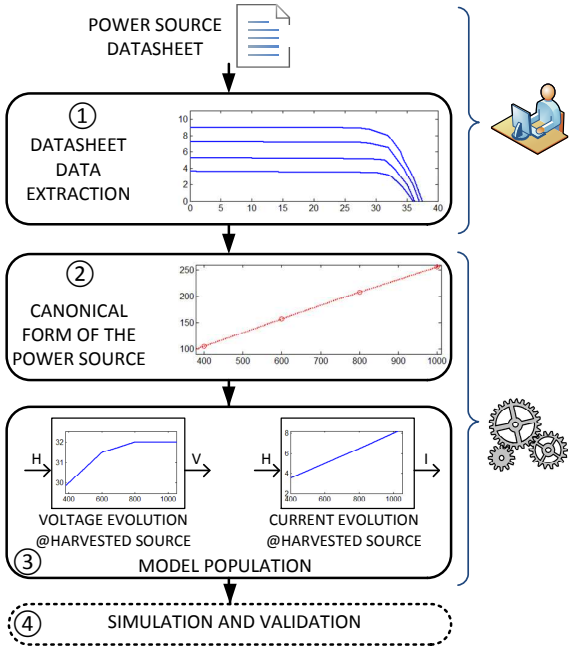

Figure 2: Proposed Modeling Methodology.

Figure 2 shows an overview of the proposed methodology. The starting point is the datasheet of the power source. The designer extracts and translates the required information into appropriate data files (step **1**). This is the only step that requires manual intervention, and it only consists of image digitation, that can be achieved almost instantaneously through automatic tools [1]. Once that the data files are filled, the canonical model of the power source is automatically constructed by casting the information in the datasheet into a function of generated power *vs.* the harvested quantity (step **2**). This step allows us to unify power source modeling and to automate the construction of model, independently of the variety of information provided by datasheets.

The canonical model is then used to automatically determine the behavior of the power source in terms of the evolution of voltage and current *vs.* time (step **3**). Finally, the model for the power source model is then inserted in an EES system for simulation and validation (step **4**).

4.2 Datasheet Data Extraction

The proposed methodology relies solely on information provided by datasheets. It was thus necessary to determine (i) how the required information are presented in typical datasheets, and (ii) how

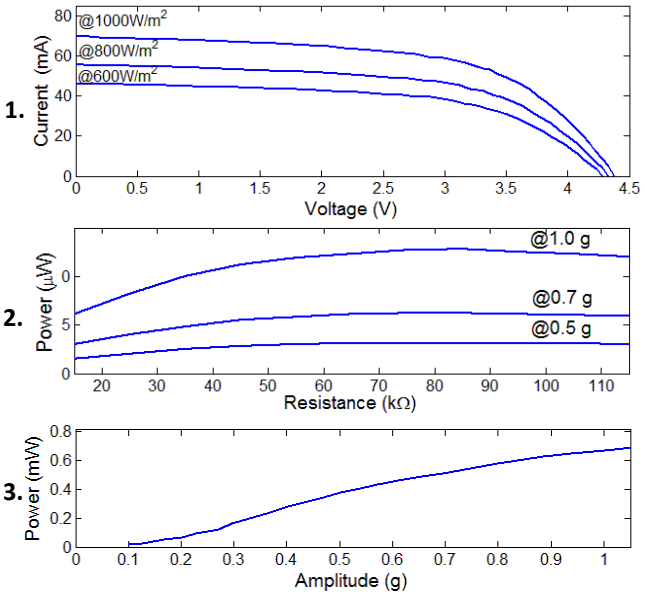

Figure 3: Examples of datasheets graphs: (1) a Class 1 graph for the photovoltaic cell in [6] (each curve is associated to a value for irradiance); (b) a Class 2 graph for the piezo-electric harvester in [4] (parameterized w.r.t. the corresponding acceleration value); (c) a Class 3 graph for the piezoelectric harvester in [3].

to represent them in a standardized file format for the automation of the methodology.

4.2.1 Analysis of Power Source Datasheets

The analysis of more than 50 datasheets for different types of power sources, including photovoltaic panels and piezoelectric harvesters, lead to the definition of three main templates.

Class 1: Current vs. *Voltage or Power* vs. *Voltage.* The most popular type of datasheets describes the characteristic behavior in terms of output current (or power) *vs.* the voltage of the power source [6, 20, 25]. An example of current *vs.* voltage graph for the photovoltaic panel in [6] is depicted in Figure 3.1. In this type of datasheets, the dependency *w.r.t.* the harvested quantity is reproduced by a number of current/voltage (power/voltage) curves, each one associated with a specific value for the harvested quantity. As an example, the curves in Figure 3.1 show the relationship between panel current and voltage for different values of solar irradiance (measured in $\frac{W}{m^2}$). Power/voltage plots are similar, since they are straightforwardly derived from current/voltage ones by multiplying voltage and current values.

Class 2: Power vs. *Resistance.* Power/resistance graphs model the power source as a family of power/resistance curves, each associated with a specific value of the harvested quantity. An example for the piezo-electric power source in [4] is shown in Figure 3.2, where power curves are parameterized *w.r.t.* the corresponding acceleration value of the oscillating mass (expressed as a multiplicative factor of g).

Class 3: Power vs. *Harvested Quantity.* Power vs. harvested quantity graphs directly explicit the dependency of power *w.r.t.* the environmental parameter. They are popular as specifications of wind power sources that operate at a fixed voltage output level, but also for some piezo-electric harvesters [2, 3, 20]. Voltage is defined in the datasheet as one or more pre-defined voltage levels, while current must be derived from the voltage and the power behavior. An example for the wind turbine in [3] is provided in Figure 3.3.

4.2.2 Definition of Data File Format

Definition of data format is an essential step for the automation of the overall methodology. Each power source is modeled with one file. The first line contains two strings representing the physical quantity associated with the x-axis and the y-axis, respectively. The strings can be any of the following: *"P"* for power, *"V"* for voltage, *"C"* for current, *"R"* for resistance and *"H"* for harvested quantity. The second line reports the number *n* of parametric values associated with the family of curves. If the graph contains one curve, n is set to 1. Else, the number n is followed by the zero-dimensional values associated to the curves. The next lines describe the curves as a list of quantized values. Each line contains *n+1* values, the first of which being the considered sampled value for the x-axis. This is followed by a number of y-axis values, describing the value assumed in correspondence to x in each curve. *E.g.*, the data file for modelling the curve in Figure 3.2 is:

R	P		
3	0.5	0.7	1.0
20,000	$19.0E-6$	$34.1E-6$	$71.3E-6$
30,000	$22.0E-6$	$44.9E-6$	$92.2E-6$
...			

4.3 Canonical Form of Power Sources

Power vs. *harvested quantity* graphs are used as the canonical form to represent power source behavior, since they conceptually represent the actual "behavior" of a power source, *i.e.*, a device that generates power according to some environmental quantity. The other two classes of graphs must thus be re-cast to the canonical form.

4.3.1 Class 1: Current/Voltage or Power/Voltage

Current *vs.* voltage and power *vs.* voltage graphs associate *a curve* to each value of the harvested quantity, thus not univocally identifying a single value of output power and voltage. Some transformations are thus necessary to reduce the current *vs.* voltage and power *vs.* voltage graphs to the canonical form. In particular, the transformation entails determining a load condition for the device.

The most typical load condition consists of trying to match the internal device resistance with that of the load, in order to extract the *maximum power point* (MPP) of the device *w.r.t.* the harvested quantity [17]. The MPP is determined by the voltage and current values that yield the maximum power for a given environmental condition. In the power *vs.* voltage graphs, the MPP for each value of the harvested quantity can be easily determined by finding the maximum of the corresponding curve. In the current *vs.* voltage graphs, the MPP is determined by reducing the graph to a power *vs.* voltage graph (*i.e.*, by multiplying voltage values per the corresponding current values). As an example, Figure 4 highlights with red circles the MPP for each irradiance value on the current *vs.* voltage graph in Figure 3.1. The canonic form can then be easily constructed by plotting the MPPs for the known values of the harvested quantity, which can be interpolated to define a continuous curve. The line with round markers on the right-hand side of Figure 4 shows the resulting canonical form for the current *vs.* voltage graph in Figure 3.1.

The values of voltage and current can be easily derived from the original current/voltage or power/voltage plot: the voltage for each value of the harvested quantity is the x-coordinate of the MPP, and the current is determined either by dividing power by voltage or by looking at the current *vs.* voltage graph.

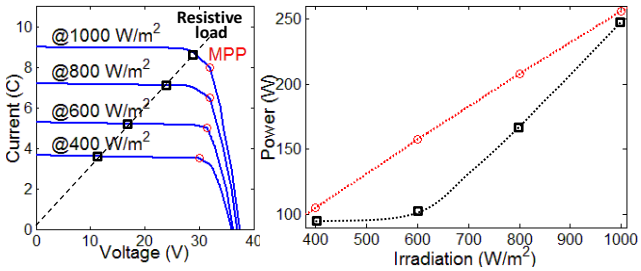

Figure 4: Canonical form of the panel in Figure 3.1, built through MPP identification (round markers) or by applying a resistive load (squared markers).

Another typical load condition would be assuming a *fixed resistive load*. This case corresponds to a line in the current/voltage graph (with slope $1/R$) or a quadratic curve ($P = V^2/R$) in the power/voltage graph. An example of linear resistive load is provided by the line with square markers on the left-hand side of Figure 4. Despite of the kind of resistive load, the curve intersects each current/voltage or power/voltage curve in exactly one point, thus determining a value for voltage (given by the x-coordinate) and a corresponding value for current. The power *vs.* harvested quantity graph is then constructed by plotting the intersection points for the known values of the harvested quantity, similarly to the case of the MPP, thus obtaining the line with squared markers on the right-hand side of Figure 4. This second case can also be used if one wants to model MPP tracking separately from the power source.

4.3.2 Class 2: Power/Resistance Characteristic

The reduction of power *vs.* resistance graphs to the canonical form follows a process similar to that of Class 1. Again, since this type of graphs associates a curve to each value of the harvested quantity rather than a single point, an identification of the load conditions is necessary. Therefore, either the MPPs of the various curves are identified in the case of matched loads, or the points intersecting a fixed resistive load (in this case a vertical line) are transposed onto the power *vs.* harvested quantity graph. Figure 5 shows the result of applying this approach to the graph in Figure 3.2, by using both the MPP approach (round markers) and a resistive load (squared markers). The corresponding voltage and current values are determined by using the voltage-current relationship $V = RI$, which allows to derive voltage and current given the power and the resistance values.

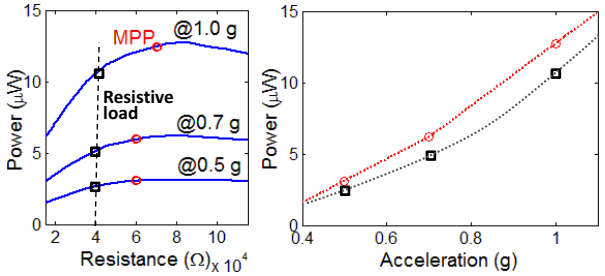

Figure 5: Canonical form of the piezo-electric harvester in Figure 3.2, built through MPP identification (round markers) or by applying a resistive load (squared markers).

4.4 Model Population

The reduction of different typologies of power sources to the canonical form allows to consider each power source as a power *vs.* harvested quantity graph that is used to automatically populate the power source model in an EES simulator. The behavior of the power source is described as a pair of curves, modeling voltage and power *vs.* the harvested quantity. The former relation is easily determined from the points used in the derivation of the latter curve (*i.e.*, the MPPs or points for a resistive load). The points are then interpolated to obtain a continuous line. Current can then be easily estimated as the ratio between power and voltage. The extraction of such information is agnostic both of the type of power source and of the scale of managed energy, and it allows to include the power source models in a wide range of simulation infrastructures, and to match requirements both on the model interface and on the system information flows [28, 29].

5. EXPERIMENTAL RESULTS

The following of this Section validates the proposed unified model for power sources, and then applies it in the context of the design of an EES system. Methodology application is automated through Matlab/Simulink R2015b.

5.1 Validation of the Proposed Unified Model

This section validates the proposed approach on power sources belonging to class **1** and class **3**, respectively. We do not show an example of class **2** power sources as they can be easily reduced to class **1** power sources. No experimental data were available for both of the power sources, and comparing the proposed model *w.r.t.* the respective datasheets would give zero error, as the models are derived from the datasheets. The methodology is thus validated against previously published and widely accepted accurate models.

5.1.1 Modeling of a Photovoltaic Panel

The power source of class **1** adopted for validation is the SunPower A300 photovoltaic panel in [26]. The datasheet models the panel through a current *vs.* voltage graph, with 4 different curves corresponding to different irradiance levels, as depicted on the left-hand side of Figure 6. We derived the corresponding canonical form by selecting the MPPs. The result is the power *vs.* irradiance graph on the right-hand side of Figure 6.

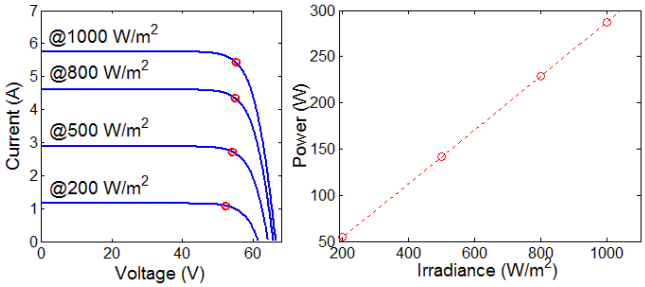

Figure 6: Datasheet specification and canonical form for the photovoltaic panel in [26].

The generated model is validated against the electrical circuit equivalent model proposed in [13], characterized for the same photovoltaic panel. Validation is performed by comparing the output power when applying the same irradiance trace, *i.e.* the irradiance in San Francisco on June 20th 2010 from 8a.m. up to 6p.m. [22].

Figure 7 depicts the evolution of the system in terms of irradiance and of correspondingly produced power. The figure shows that the produced power (middle) is directly proportional to the received irradiance (top). The center figure compares also the power resulting from our model (dashed lines) against the values provided by the circuit model of [13] (solid lines). The two curves are almost totally overlapped. For a better quantification of error, the bottom plot

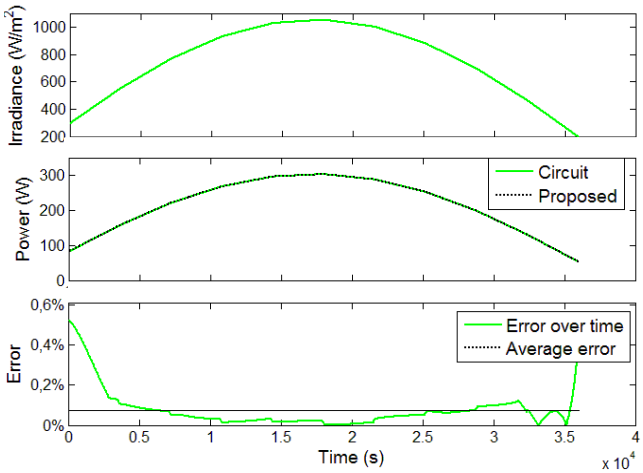

Figure 7: Model Validation of the A300 Panel: irradiance over time (top), power over time with the two models, (center), and error committed by the proposed approach *w.r.t.* the circuit model (bottom).

of Figure 7 reports the sample-by-sample error between our model and the one of [13]; average error is extremely low, *i.e.* 0.075% (dashed line). Overall, error is always below 1% (solid line), with maximum error 0.52%. This confirms that the proposed approach allows to accurately model power sources. The bottom plot of Figure 7 also highlights that error tends to be larger at the beginning and at the end of simulation time, where irradiance is about $200\frac{W}{m^2}$. This is due to the almost linear growth (reduction) of irradiance in the corresponding time slots. Furthermore, the datasheet does not provide any trace for irradiance values lower than $200\frac{W}{m^2}$ (as in Figure 6). This may induce errors in the interpolation process, and thus the estimation of the produced power becomes less accurate.

It is worth emphasizing that the model in [13] must be populated with detailed characteristics of the panel, *e.g.*, open-circuit and short-circuit characteristics and technology specific coefficients. On the contrary, a major advantage of the proposed approach is that panel behavior is inferred only from the available datasheet information. A further advantage is that our model took only 1.363s to compute the whole simulation, with a 7.707x speedup *w.r.t.* the circuit model, whose simulation lasted 10.505s.

5.1.2 Modeling of a Wind Turbine

Multiphysics-based mechanical models are amongst the most accurate models for power sources. For this reason, we decided to validate the proposed approach against the wind turbine model described in [27], based on a stator-flux-oriented electromechanical model of a doubly fed induction machine.

We first implemented the approach in [27] in Matlab/Simulink and we configured it for simulating the WT2000 wind turbine [3]. It is important to note that this configuration step was challenging, as it required to acquire very detailed information about the wind turbine, both by analysing the specifications and through physical measurements. As a next step, we reproduced the same wind turbine by adopting the approach proposed in this work. The datasheet provides a power *vs.* wind curve (depicted in Figure 3.3), that was extracted and used as canonical form for our power source.

Figure 8 shows the evolution of output power given the same wind trace for both models, *i.e.*, the wind traced at Long Island on February 03rd 2005 [22]. The figure shows that the produced power (bottom) reflects the observed wind (top). The middle figure also compares the approach proposed in this work (dashed lines) with the mechanical model (solid lines).

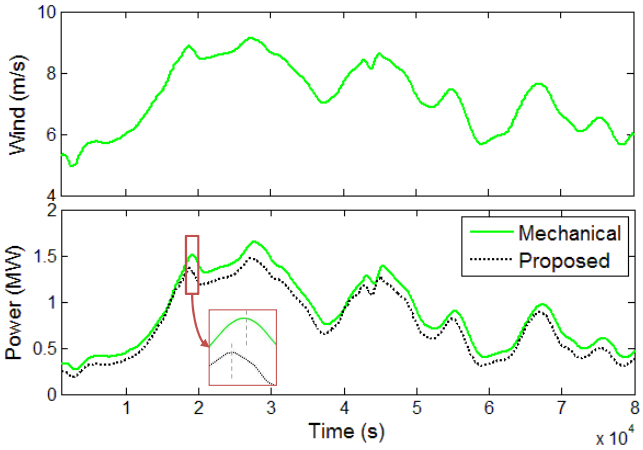

Figure 8: Validation of the modeling of a wind turbine *w.r.t.* the multiphysics-based model in [27].

It can be noted that this case study exposes a lower level of accuracy *w.r.t.* the previous one. The proposed approach underestimates the mechanical model, with *avg.* error of 11.09% and maximum error 21.88%. On the other hand, [15] showed that the mechanical model, hereby used as reference, tends to overestimate the actual generated power, even if no accurate statistics were provided. Thus, the error is not entirely caused by the proposed approach, as it is compared *w.r.t.* an inherently approximate model, rather than with experimental results.

The accuracy of the model proposed in this work is also granted by the fact that datasheet plots, used for the construction of the model, are built based on experimental measurements. As a result, the model adheres to the actual behavior of the wind turbine. On the contrary, mechanical models tend to deepen mechanical aspects and to lose accuracy on complex physical mechanisms, such as practical mechanical losses, or factors impacting on the energy conversion. Thus, the error can not be ascribed only to the model proposed in this work, but it is generated by the adjunct approximations of both the proposed model and the mechanical one.

A limitation of the proposed approach is that the generated model does not keep into account delays caused by the inherent mechanical inertia of the turbine. This is highlighted by the zoom-in in Figure 8: our model reacts instantaneously to changes in the wind speed, while the mechanical model delays the response of power generation. This could be easily avoided by determining the delay timing constant, *e.g.*, by extracting it from the mechanical model, and by adding a moving-average filter just after the canonical model. This analysis will be part of future work.

5.2 Using the Unified Model for System Level Simulation

This section demonstrates that the proposed system-level abstract model for power sources allows one to implement an explorative analysis using in-the-loop simulation of different configurations for realistic time durations in the order of a few weeks. Running such an experiment using detailed mechanical or circuit models of the power sources would be prohibitive, as a day-long simulation would be too costly in terms of memory and time.

Specifically, we model an EES featuring a SunPower A300 PV panel [26] (as in Section 5.1.1) and a Dolphinz Z-300w wind turbine, with a rated power of 300W [12]. The energy storage consists of a pack of Li-ion batteries built from a cell by Qinetiq with capacity of 5.8Ah. The system includes also the necessary DC-DC converters and a CTI bus.

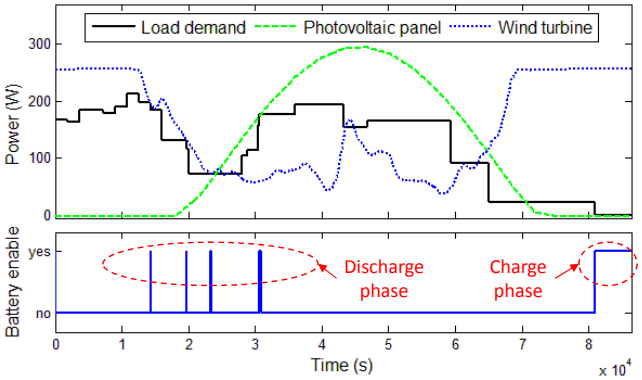

Figure 9: Adoption of the canonical models of a photovoltaic panel and a wind turbine in an example EES: evolution of load demand and power sources production over time (top), and corresponding activation of the battery pack (bottom).

The system is managed by a charge allocation policy that operates as follows: As long as the the power drawn from the power sources satisfies the loads power demand, loads are supplied directly by the power sources. Otherwise, loads are supplied by the battery pack, until the state-of-charge (SOC) is below 10%. Finally, the battery is charged whenever load power demand is 0. Although this policy is sort of naive, the focus here is not to develop sophisticated policies but rather to show the effectiveness of the proposed canonical model for power sources.

To estimate the correct sizing of the battery pack, we evaluated the EES with three different capacities (*i.e.*, 200Ah, 320Ah and 440Ah). Each simulation reproduces one month of simulated time, with variable irradiance and wind values. To emulate the variance in irradiance we assumed about 1/3 of cloudy days and 2/3 of sunny days. For wind speed, we used a typical daily profile taken from published data [14, 15], with small perturbations at random time points in the different days.

Figure 9 depicts the typical trace over one (sunny) day, in terms of load demand and power produced over time by the PV panel and the wind turbine (top). The Figure shows also the activation of the battery pack *w.r.t.* the policy (bottom), either to provide power to the loads when power sources production is insufficient (activations 1–4) or to charge the battery (activation 5).

Each simulation (three 1-week runs) lasted in average 767.04s. Table 1 reports minimum and average SOC and average residual SOC at midnight (after the charge phase) of the three configurations. The best configuration is obviously achieved with largest capacity (440Ah), which guarantees an almost complete recovery of battery SOC during the day. However, the designer may use this analysis to determine a cost-benefit tradeoff, *e.g.*, to choose a target minimum or average daily SOC level and choose the capacity configuration that satisfies that constraint.

Battery Capacity (Ah)	Min. SOC (%)	Avg. SOC (%)	Avg. SOC at midnight
200	60.22	91.05	86.18
320	76.65	94.66	91.82
440	83.52	96.21	94.21

Table 1: Effect of variation of the battery pack capacity over the evolution of SOC over time.

6. CONCLUSIONS

This work proposed a unified model for power sources, built solely from the information available in their datasheet specifications, with the goal of providing designers with a system level model and of easing EES simulation and validation. The proposed methodology is entirely automatic, despite of data extraction from the provided datasheet. The proposed approach allows thus early simulation of power sources and EES without empirical measurements, still guaranteeing a good approximation of the power source behavior. Experimental results showed that the proposed approach reaches a high level of accuracy *w.r.t.* widely accepted accurate models, together with a simulation speed up of up to 7x. Furthermore, the proposed model proved to enhance EES design with instantaneous system modeling and simulation. Future work will support dependency from other environment characteristics, such as temperature and humidity.

7. REFERENCES

[1] S. A. van der Wulp. *Graph Digitzer*. www.mathworks.com/matlabcentral/fileexchange/23317-graph-digitzer.

[2] AMSC. *SeaTitan 10 MW Wind Turbine*. www.amsc.com.

[3] AMSC. *WindTec wt2000df and wt2000fc*. www.amsc.com.

[4] R. Andoscaa, T. McDonald, et al. Experimental and theoretical studies on MEMS piezoelectric vibrational energy harvesters with mass loading. In *Sensors and Actuators A: Physical*, volume 178, pages 76–87. Elsevier, 2012.

[5] A. Bauer, J. Hanisch, and E. Ahlswede. An Effective Single Solar Cell Equivalent Circuit Model for Two or More Solar Cells Connected in Series. *IEEE PHOT*, 4(1):340–347, Jan 2014.

[6] Canadian Solar. *CS6P-250 255 260P Datasheet*. www.mitsubishielectric.com.

[7] COMSOL. *COMSOL Multiphysics*. www.comsol.com.

[8] Coventor. *CoventorWare MEMS Design*. www.coventor.com.

[9] J. Eker, J. Janneck, E. Lee, et al. Taming heterogeneity - the Ptolemy approach. *Proc. of the IEEE*, 91(1):127–144, Jan 2003.

[10] M. A. Faruque and F. Ahourai. A Model-Based Design of Cyber-Physical Energy Systems. In *Proc. of IEEE ASPDAC*, pages 97–105, 2014.

[11] P. Fritzson. *Introduction to Modeling and Simulation of Technical and Physical Systems With Modelica*. Wiley-IEEE Press, 2011.

[12] GoGreenSystems. *Doplphinz 300 Z-300w wind turbine*. gogreensystems.se.

[13] F. Gonzalez-Longatt. Model of Photovoltaic Module in Matlab. In *Proc. of CIBELEC*, pages 1–5, 2005.

[14] K. Heussen, S. Koch, A. Ulbig, and G. Andersson. Unified system-level modeling of intermittent renewable energy sources and energy storage for power system operation. *IEEE SJ*, 6(1):140–151, March 2012.

[15] M. Hurajt. Simulation of a wind energy conversion system utilizing a vector controlled doubly fed induction generator. Technical report, University of Windsor, 2013. scholar.uwindsor.ca/etd/4979.

[16] M. Ilic, L. Xie, U. Khan, and J. Moura. Modeling future cyber-physical energy systems. In *IEEE PES General Meeting*, pages 1–9, July 2008.

[17] D. Karanjkar, S. Chatterji, et al. An improved current feedback based maximum power point tracking controller for solar photo-voltaic system. In *Proc. of IEEE AICERA/ICMiCR*, pages 1–6, 2013.

[18] Y. Kim, D. Shin, et al. Computer-aided design of electrical energy systems. In *Proc. of IEEE ICCAD*, pages 194–201, 2013.

[19] C. Lu, V. Raghunathan, and K. Roy. Efficient design of micro-scale energy harvesting systems. *IEEE ETCAS*, 1(3):254–266, Sept 2011.

[20] MIDE. *Volture EHE004 Datasheet*. www.mide.com.

[21] J. M. Morales et al. Integrating renewables in electricity markets. In *International Series in Operations Research & Management Science*, 205. Springer, 2014.

[22] National Renewable Energy Laboratory. *Leading Clean Energy Innovation*. www.nrel.gov.

[23] P. Palensky, E. Widl, and A. Elsheikh. Simulating cyber-physical energy systems: Challenges, tools and methods. *In Proc. of IEEE SMC*, 44(3):318–326, 2014.

[24] M. Singh and S. Santoso. Dynamic Models for Wind Turbines and Wind Power Plants. Technical report, National Reneawable Energy Laboratory, May 2011. www.osti.gov/bridge.

[25] SpectroLab. *GaAs/Ge Single Junction Solar Cells Datasheet*. www.spectrolab.com.

[26] SunPower. *300 Solar Panel*. www.energymatters.com.au.

[27] G. Tapia, A. Tapia, and J. Ostolaza. Two alternative modeling approaches for the evaluation of wind farm active and reactive power performances. *IEEE EC*, 21(4):909–920, Dec 2006.

[28] The MathWorks, Inc. *SimPowerSystems - Model and simulate electrical power systems*. mathworks.com.

[29] S. Vinco, A. Sassone, et al. An open-source framework for formal specification and simulation of electrical energy systems. In *Proc. of IEEE/ACM ISLPED*, pages 287–290, 2014.

[30] S. Yue, D. Zhu, et al. SIMES: A Simulator for Hybrid Electrical Energy Storage Systems. In *Proc. of ACM/IEEE ISLPED*, pages 33–38, 2013.